Adaptive Finite Element Methods for Distributed Parameter System Identification: Applications in Fluorescence Enhanced Frequency Domain Optical Tomography

Amit Joshi and Eva M. Sevick-Muraca
Photon Migration Laboratories
Texas A & M University
College Station, TX 77843-3573
email: eva-m-sevick@tamu.edu

Abstract— This article addresses the distributed parameter system identification problem encountered in fluorescence enhanced optical tomography. Adaptive mesh refinement techniques can increase the efficiency of estimation algorithms by reducing the computational storage as well as tailoring the solution strategy to the problem structure. An adaptive refinement based Galerkin finite element scheme for coupled photon diffusion equations is implemented with a simply bound limited memory quasi-Newton algorithm, which is suitable for large scale nonlinear optimization. The efficacy of the proposed scheme is demonstrated on two dimensional test cases.

I. INTRODUCTION

The success of human genome project has paved the way for the complete characterization and quantization of biological processes at the molecular level. The ability to molecularly target therapeutic agents to specific disease markers (such as Herceptin receptors in breast cancer [1]), has spawned an urgent need for a clinical, diagnostic imaging technique for selection of appropriate molecular therapies. Fluorescence enhanced optical tomography is a novel functional imaging modality which is well suited for molecular imaging of targets in nanomolar tissue concentrations [2]. The tomography problem itself involves identification of a distributed parameter involving the recovery of the interior optical property map from the knowledge of the source distribution and a sampling of the boundary measurements, that satisfies a coupled system of elliptic partial differential equations. This is an ill-posed inverse problem. Finite element simulations of light transport in the tissue constitute the bulk of computational requirements for the parameter estimation algorithms. A fine discretization improves the quality of the simulation but at the same time increases the ill-posed ness of the inverse problem by increasing the number of unknown parameters to be estimated. In this article we propose a novel algorithm which couples adaptive finite element meshing schemes with large scale non-linear optimization algorithms for computationally efficient and stable solution of the fluorescence tomography problem.

II. MATHEMATICAL MODEL FOR LIGHT TRANSPORT IN TISSUE

In fluorescence enhanced frequency domain optical tomography a sinusoidally modulated Near Infrared laser light source is applied to the boundary of the domain. The light propagates diffusively throughout the domain and upon encountering a fluorescently tagged target is absorbed and produces fluorescent light. The modulated fluorescence light is detected at the boundary of the domain (Figure-1). The amplitude and phase of fluorescent wave can be predicted by the coupled diffusion equations [3].

$$-\nabla \cdot [D_x(\mathbf{r})\nabla \Phi_x(\mathbf{r},\omega)] + [\frac{i\omega}{c} + \mu_{axi}(\mathbf{r})$$
$$+\mu_{axf}(\mathbf{r})]\Phi_x(\mathbf{r},\omega) \quad = 0 \qquad (1)$$

$$-\nabla \cdot [D_m(\mathbf{r})\nabla \Phi_m(\mathbf{r},\omega)] + [\frac{i\omega}{c} + \mu_{ami}(\mathbf{r})$$
$$+\mu_{amf}(\mathbf{r})]\Phi_m(\mathbf{r},\omega) = \phi\mu_{axf}\frac{1}{1-i\omega\tau}\Phi_x(\mathbf{r},\omega) \qquad (2)$$

where Φ is the complex photon fluence of the excitation or emission radiation. $\Phi = Iexp(-i\varphi)$. I is the amplitude (photons/cm^{2}s) and φ is the phase shift relative to incident excitation light; 'x' stands for NIR excitation and 'm' for fluorescent emission; $D_{x,m}$ (cm) is the optical diffusion coefficient at excitation and emission wavelength; c is the velocity of light in the media; $\mu_{ax,mi}$ (cm^{-1}) is the absorption owing to natural chromophores; $\mu_{ax,mf}$ (cm^{-1}) is the absorption due to fluorophores; ω is the angular modulation frequency(rad/s); ϕ is the quantum efficiency of fluorescent emission and τ is the lifetime(ns) of the fluorophores. Equations (1) and (2) are solved with the Robin boundary conditions:

$$2D_{x,m}\frac{\partial \Phi_{x,m}}{\partial n} + \gamma\Phi_{x,m} + S\delta(\mathbf{r},\mathbf{r}_s) = 0 \; on \; d\Omega \qquad (3)$$

Where n denotes the outward vector normal to the surface. In the fluorescence tomography problem considered in this contribution all the parameters except μ_{axf} are considered to be known. The distribution of μ_{axf} over the entire domain is identified from the boundary emission fluence measurements.

III. INVERSE PROBLEM

In the fluorescence tomography problem considered in this contribution all the parameters except μ_{axf} are considered to be known. The image reconstruction problem involves
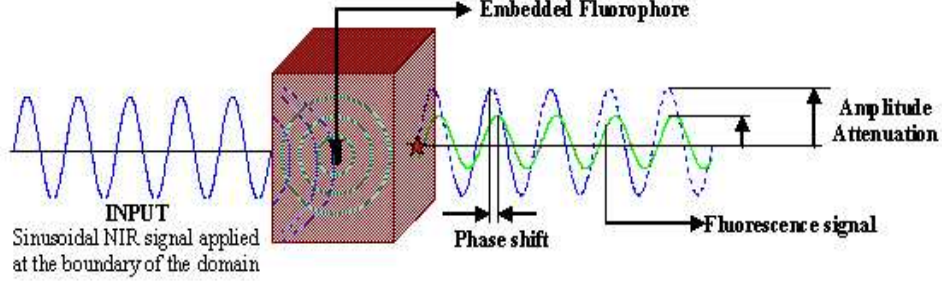
Fig. 1.   Figure-1

identification of μ_{axf} distribution over the entire domain from the boundary emission fluence measurements. This inverse problem is formulated as a simply bound constrained minimization problem:

min $E(x)$ $\forall$ x s.t $lb \leq x \leq ub$

$$E(x) = \left\| \frac{Ax - z}{z} \right\|_2^2 \qquad (4)$$

Here x is the unknown parameter to be estimated which is in our case. The term z denotes the experimentally measured boundary fluorescence fluence distribution and A denotes the elliptic operator defined by equations (1) and (2) which maps the optical property distribution onto the boundary fluorescence fluence distribution. The terms lb and ub denote the lower and upper bounds on x which are assumed known. In practice a finite number of boundary measurements are made for each source position. The error functional can then be written as:

$$E(x) = \frac{1}{2} \sum_{i=1}^{ns} \sum_{j=1}^{nd} \left(\frac{Ax_{ij} - z_{ij}}{z_{ij}} \right) \left(\frac{Ax_{ij}^* - z_{ij}^*}{z_{ij}^*} \right) \qquad (5)$$

Here 'ns' denotes the number of excitation sources and 'nd' denotes the number of boundary measurements made for each source. Before the minimization can be carried out, the parameter distribution and the state equations described by the system of equations (1) need to be discretized. Galerkin finite element scheme is employed for this purpose [3]. We propose a novel scheme with separate finite element meshes for the parameter and the state equation solver. Both the meshes are adaptively refined to ensure optimality of the state equation solution and control of resolution in image reconstruction process while at the same time minimizing the computational effort.

IV. ADAPTIVE FINITE ELEMENT MESH REFINEMENTS FOR INVERSE PROBLEM

A. State Equation Discretization

The minimization routine iteratively updates the interior μ_{axf} map. Determination of these updates requires repeated solution of the coupled diffusion equations (1) and (2). We have employed the Galerkin finite element method. The problem domain is subdivided into triangular finite elements. A finer mesh ensures more accurate solution, however mesh needs to fine only where the error in solution is larger but the exact solution is unknown. This creates a need for the generation of a posteriori error estimates which identify the triangles to be refined once a trial solution has been computed on a coarse mesh. Solution process is started with a coarse mesh and the successive meshes are generated according to the a posteriori error estimator. To develop the error estimates for coupled diffusion equations we have followed the procedure developed by Kelly [4] and Salazar-Palma [5]. Kelly's error estimator is a residual based energy norm estimator which essentially refines the mesh where the gradient of the solution shows rapid variation. The error for each triangular element is calculated by the following equation:

$$\in_e^2 = \alpha_e \int_{\Omega^e} r_s^2 d\Omega + \beta_e \sum_{\Gamma_k \subset \Gamma_{\Omega^e}} \int_{\Gamma_k} r_{ed}^2 d\Gamma \qquad (6)$$

Here r_s and r_{ed} are the surface and lumped edge residuals of the intra-element and inter-element photon fluence flux densities. α_e and β_e are weighing factors depending upon the triangle dimensions. The global error for the finite element mesh is determined by summing the local error for all the elements:

$$\|e\|_\Omega^2 = \sum_{e=1}^{N_e} \in_e^2 \qquad (7)$$

If global error is greater than a predefined threshold the mesh is refined then the mesh is refined wherever the local error is greater than 50% of the maximum error, that is if

$$\frac{\in_e^2}{max(\in_e^2)} \geq 0.5 \qquad (8)$$

The triangles which were marked to refined were subdivided into four triangles. To maintain the continuity of the mesh neighboring triangles are also refined to some degree.

V. PARAMETER DISCRETIZATION

The unknown parameter x is also discretized on a separate triangular mesh which is coarser than the state equation mesh to ensure that the inverse problem is well posed. The parameter mesh is adapted when the error function has

converged on the coarser mesh. This refinement is driven by the jump in the reconstructed unknown parameter. In effect this refines the mesh at the boundaries of the fluorescent heterogeneity embedded in the domain and thus improves the resolution of the reconstructed image only where needed. The refinement criteria we have used is inspired by the work of Molinari et al [6] in electrical impedance tomography. The elemental error estimate for the parameter mesh estimates the smoothness of the parameter distribution. It is given by:

$$\in_e^p = \sum_{edges} |log(x_i) - log(x_j)| \, l_{ij} \qquad (9)$$

Where l_{ij} is the length of the edge separating element i and element j. x_i is the value of the parameter in the triangle i. The criterion described in equation (8) is used to determine the triangles to be refined.

VI. INVERSION ALGORITHM

We have employed the limited memory BFGS method with simply bound constraints [7] to carry out the minimization of the error functional. Limited memory BFGS method is a quasi-Newton optimization method which approximates the second derivative of the error function by storing the gradients of error function at previous five iterates. This results in a robust and memory efficient algorithm. The quasi-Newton update for the μ_{axf} map is given by

$$\mu_{axf}^{k+1} = \mu_{axf}^k - \alpha^k (H^k)^{-1} g^k$$

Here g^k is the gradient of the error function evaluated at kth iterate. The gradients of the error functional are constructed by an ad joint differentiation scheme [3] employing the finite element discretization of the state equations; H^k is the Hessian matrix of the error function at the current iterate. It is approximated by the following expression:

$$H^{k+1} = (I - \rho s_k y_k^T) H^k (I - \rho y_k s_k^T) + \rho s_k s_k^T$$

Where $s_k = \mu_{axf}^{k+1} - \mu_{axf}^k$
$y_k = g_{k+1} - g_k$
The number of vectors k stored can be varied according to the dimensions of the problem. We have gotten optimal results with $k = 5$. The term α^k is the step length which is determined by the line search procedure of More and Thuente [8]. We have used the information about lower and upper bounds of μ_{axf} in determining the update direction. This helps in minimizing computational costs and ensuring feasible solutions. When the error function converges on a given mesh, the meshes for the state and parameter variables are refined. This process is continued till there is no further decrease in error function.

VII. IMPLEMENTATION AND RESULTS

The inversion process is outlined above was tested with synthetic measurement data generated on a two dimensional domain. The domain used is an ellipse with a fluorescent heterogeneity embedded in the middle (Figure-2).
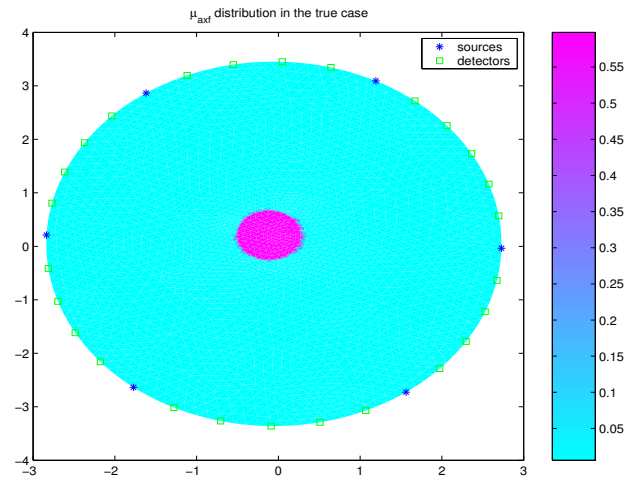

Fig. 2. Domain used for generating synthetic data

The optical properties are fixed to have a fluorescence absorption contrast of $100 : 1$ in the embedded heterogeneity with respect to the background. Six sources and twenty six detectors for each source are used. To generate the boundary fluorescence fluence measurements the coupled diffusion equations were solved on a very fine finite element mesh with 2257 nodes and 4384 triangles. The reconstruction algorithm started with coarse meshes (154 nodes) for the state and the unknown parameter (fluorescence absorption coefficient) and the meshes were adaptively refined during the iterations of the limited memory BFGS method. The final solution was obtained in 250 iterations. The final state mesh contained 751 nodes and the parameter mesh contained 401 nodes.Figure-3 shows the reconstructed image.

A substantial accuracy was attained in the state equation solution as the global solution error was matched with a 2257 node mesh with only 751 nodes.In the parameter mesh, maintaining a separate adaptable discretization helped in keeping the number of unknowns to 401 while still providing a finer resolution at the boundary of the heterogeneity.

The efficiency achieved by adaptive finite element schemes is demonstrated in figure-4 which compares the decrease in global error (7) attained by adaptive mesh refinement with that attained by uniform global refinement.

To reduce the global error to a level equivalent to global refinement, adaptive refinement requires an order of magnitude less number of nodes. This results in a two order of magnitude saving in the computational cost of the algorithm.Figure-5 shows the evolution of the state and parameter meshes. MATLAB's PDE Toolbox was used to generate and adaptively refine the finite element meshes for these contributions.
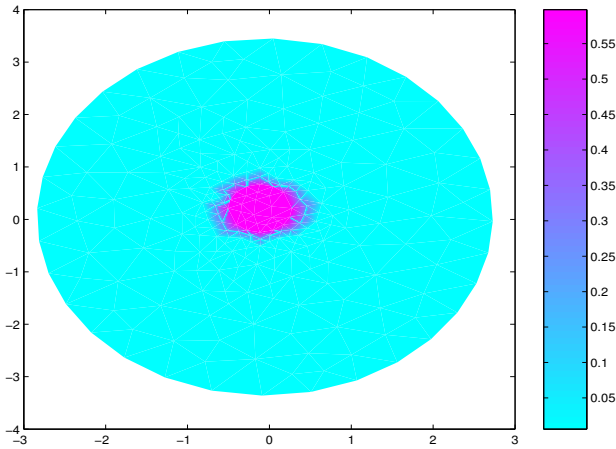
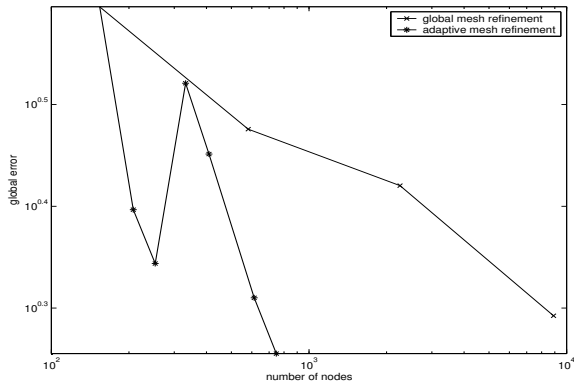Fig. 4.   Recovered μ_{axf} map

Fig. 5.   Global error decrease with adaptive and uniform refinement

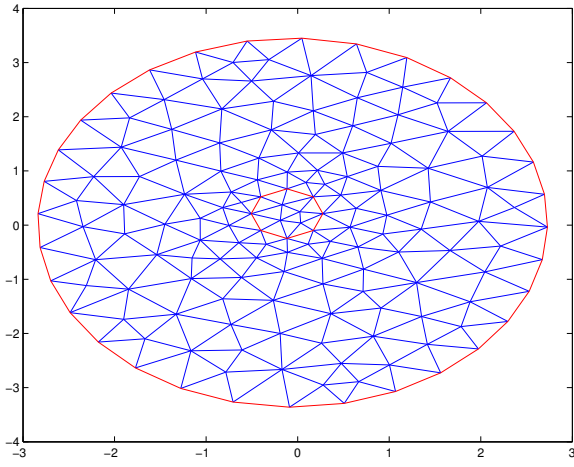## VIII. CONCLUSIONS AND FUTURE WORK

We have demonstrated a novel approach to handle large dimensional ill-posed system identification problems for distributed parameter systems with adaptive finite elements. The approach can be readily transformed for handling three dimensional systems provided sophisticated tools for handling three dimensional meshes are available. Currently work is underway on applying these techniques for three dimensional problems and on working with actual experimental data obtained in the photon migration laboratories.
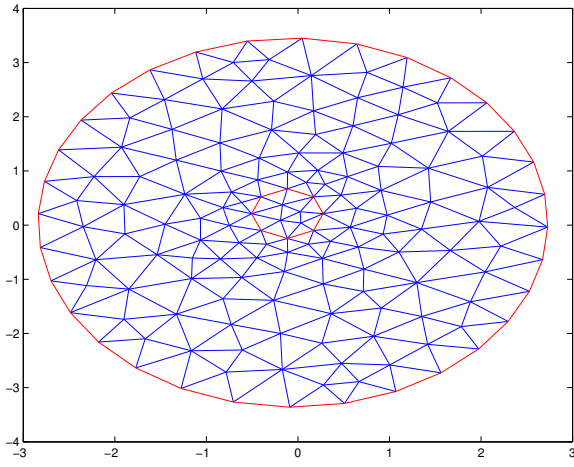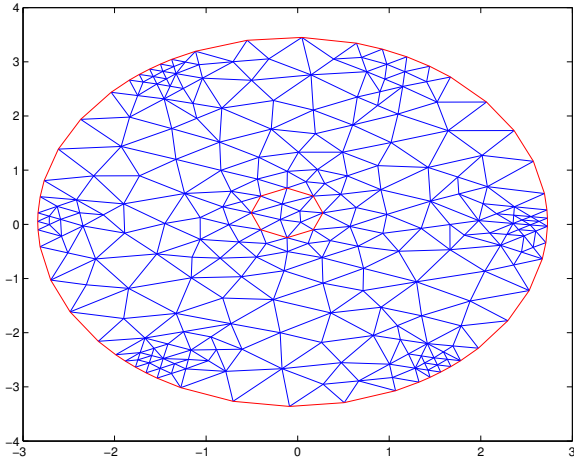
IX. ACKNOWLEDGMENTS

X. REFERENCES

[1] I.E. Smith. Efficacy and safety of herceptin (r) in women with metastatic breast cancer: results from pivotal clinical studies. *Anti-Cancer Drugs*, 12:S3–S10, 2001.

[2] J.P. Houston, A.B. Thompson, M. Gurfinkel, and E.M. Sevick-Muraca. Sensitivity and penetration depth of nir fluorescence contrast enhanced diagnostic imaging. *Photochem. Photobiol*, 77(4):77–103, 2003.

[3] R.Roy and E.M.Sevick-Muraca. Truncated newton's optimization schemes for absorption and fluorescence optical tomography :part(1) theory and formulation. *Optics Express*, 4:353–371, 1999.

[4] D.W.Kelly, S.R.J.P. Gago, O.C Zienkiewicz, and I. Babuska. A posteriori error analysis in finite element method: Part i–error analysis. *Int. J. Numer. Math. Eng*, 19:1593–1619, 1983.

[5] Magdelena Salazar-Palma, Tapan K Sarkar, L.E.G. Castillo, and A. Djordjevic. *Iterative and Self Adaptive Finite Elements in Electromagnetic Modeling*. Artech house, Norwood,MA, 1998.

[6] Marc Molinari, Barry H. Blott, Simon J. Cox, and Geoffrey J. Daniell. Adaptive mesh refinement techniques for electrical impedence tomography. *Physiological Measurement*, 22:91–96, 2001.

[7] Jorge Nocedal and Stephen J. Wright. *Numerical Optimization*. Springer-Verlag, 1999.

[8] J.J. More and D.J. Thuente. Line search algorithms with guaranteed sufficient decrease. *ACM Trans. Math. Software*, 20:286–307, 1994.
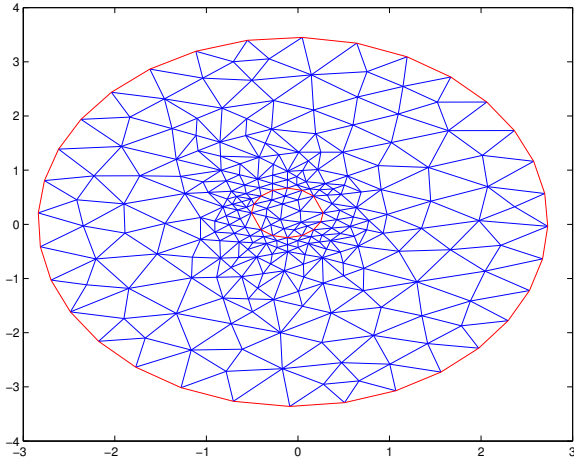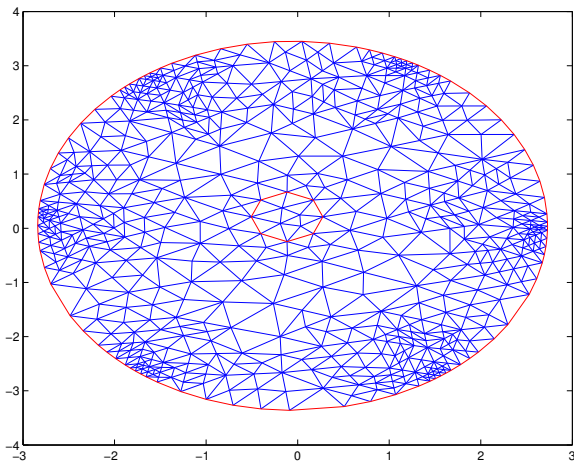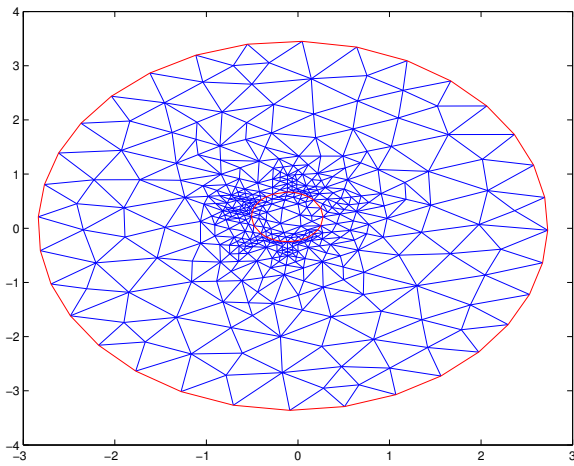
(a)

(b)

(c)

(d)

(e)

(f)

Fig. 3.   Self Adaptive Mesh evolution for State and Parameter Discretization